High configurational entropy: Strategy to design P2-type layered oxide cathode for Na-ion batteries

*Amrapali Patil [1], Sagar Mitra[2]**

[1, 2] *Energy Science and Engineering Department Electrochemical Energy Laboratory (ECEL)*

IIT Bombay, Maharashtra, 400076, India

(*sagar.mitra@iitb.ac.in)

Abstract

Recent advances in renewable energy have increased the demand for efficient electrical energy storage technologies, driven by global energy needs and climate change concerns. With nearly two billion people lacking access to reliable electricity, energy storage devices are crucial, especially for integrating renewable sources into local grids. Li-ion batteries, however, are the most advanced technology, limited lithium resources make them unsustainable for large-scale deployment. Na-ion batteries provide a promising substitute because of the presence of sodium and low cost. In Na-ion batteries, cathode materials are critical, as they account for a greater mass fraction than anodes and significantly influence the battery's cost, safety, capacity, and energy density. Among potential cathode candidates, P2-type $Na_{0.67}Ni_{0.33}Mn_{0.67}O_2$ is particularly attractive due to its simple synthesis, high operating potential (~3.5 V vs. Na/Na^+), theoretical capacity (173 mAh g^{-1}), and specific capacities exceeding 140 mAh g^{-1}. Additionally, its P2 structure enables faster Na^+ ion transport than O3-type counterparts. However, its practical use is hindered by capacity fading and limited cycle life. To address these issues, the high entropy material strategy provides a new avenue for cathode development. The generic thought is to maximize the configurational entropy of the system to stabilize the single phase. By tuning the entropy of the system with multiple elements, a more flexible system can be achieved, which is found to be advantageous in increasing the specific capacity, energy density, and reversibility. This review proposes designing P2-type layered oxide cathodes using high configurational entropy to develop advanced, stable, and high-capacity materials for next-generation sodium-ion batteries.

Keywords: *Energy storage device, Na-ion batteries, P2-type layered oxide cathode, high configurational entropy.*

1. Introduction

Na-ion batteries (NaBs) have garnered significant interest in academic excellence and commercial industrial sectors since the 2000s. They offer several advantages that make them a compelling alternative or complement to lithium-ion batteries. NaBs are low-cost, environmentally friendly, have a reduced supply risk in the future, and are considered safer, making them a promising alternative for various applications [1–3]. There are plenty of merits to NaBs but are still tough to commercialize due to their limitations. **Figure 1** shows the schematic representation and mechanism of Na^+-ion (de)/insertion during charging and discharging. During charging, an oxidation event involving Na^+-ions (de)/insertion and electron (e^-) loss takes place at the cathode (e.g. Na_xMnO_2). In this process, e^- moves from the outer circuit and Na^+-ions move through the internal pathway (i.e. electrolyte) to the anode (e.g. hard carbon). During discharge opposite process happens where Na^+-ions are inserted at the cathode as a result, a reduction reaction takes place [4]. The ideal battery should be defined with a lower cost, reliable safety, high energy density, long-term cycling life, and large specific power, especially for grid energy storage and portable electronic devices [4]. As of right now, some significant anode materials show specific capacities of 300–600 mAh g^{-1} and operating potentials of 0.1–0.6 V (close to the potential of Na plating) [5–7], while cathode materials show specific capacities of 120–200 mAh g^{-1} and operating potentials of 2.6–3.2 V (much lower than the oxidation potential of electrolytes, >4.0 V) [8–10]. Moreover, due to the low gravimetric and volumetric energy densities of positive

electrode material for NaBs which are not sufficient to reach up to the capacities of negative electrode material, it is difficult to achieve broader voltage windows which some extent hinders the commercial expansion of NaBs in the next-generation energy storage devices [1,4]. In addition, it occupies a larger mass fraction and bigger space in the battery after mass balancing with the anode capacity.

The overall performance in terms of cost, safety, specific energy, cycling life, and specific power is greatly influenced by cathode material selection. Therefore, cathode materials exhibit attention for increasing the NaBs voltage window.

Structural stability in the high voltage range determines the cathode's longevity with the electrochemical stability of the electrolyte [4]. The main limiting factor for the large-scale application is the poor performance and slow reaction kinetics at low temperatures [11,12]. The slow movement of Na^+-ion at low temperatures reduces the capacity of the battery, other is the phase transition [13], and irreversible lattice anionic redox affects the structural integrity that results in the transition metal migration (i.e. cation) and lattice distortion leads to severe voltage decay and poor cycling performance [14,15].

This review article summarizes the advances of high configurational entropy (HCEs) in NaBs. Recently, HCEs raised significant attention towards particular uses for energy storage in rechargeable batteries. The combination of various elements in the system gives rise to tailorable properties and opens up opportunities for creating high-performance batteries [16–18]. Generally, we know that entropy is the degree of randomness, which creates a lot of confusion in explaining the high entropy materials (HEMs). Here, we focus on understanding the definition of HCEs which clarifies the differences between configurational entropy (CE) and randomness in the structure. Also, we aim to propose HCEs, a strategy to develop highly efficient cathodes for NaBs that offers new opportunities to address the challenges associated with P2-type layered oxide cathodes.

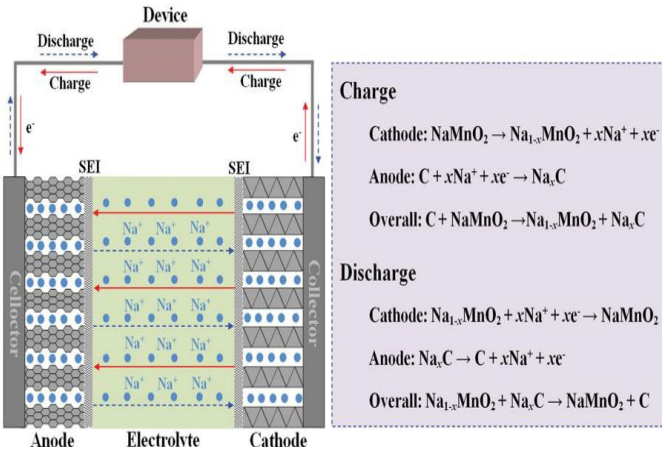


Figure 1. Schematic representation and Na+-ion (de)/ insertion mechanism in NaBs [ref. 4].

2. Layered oxide material

Various cathode materials were discovered in recent years which include oxides, among the various materials studied for NaBs, polyanionic compounds, Prussian blue, and organic compounds have shown significant potential. However, layered oxide materials are considered one of the leading contenders for practical industrial applications. This is due to their high structural balance with reversible Na^+ (de)/intercalation chemistry, which is crucial for efficient energy storage and retrieval in NaBs.

The framework of layered oxide material is made up of oxygen anions which were arranged in a hexagonal closed packing, the two layers of anions form alternate octahedral and tetrahedral voids, and the transition metal ion is present in the octahedral void, tetrahedral voids remain empty. This is known as an MO_2 slab, (where M-represents the transition metal) these MO_2 slabs are arranged parallelly and form a layered structure. In between the two MO_2 slabs, there is a space known as interlayer spacing which acts as a host for Na^+-ions, shown in **Figure 2 (a-e)**. Based on the oxygen anionic packing, two types of interlayer spaces were formed: prismatic and octahedral thus layered oxide material is classified as P2, P3, O2, and O3 type, P stands for prismatic void and O stands for octahedral void which is the environment of Na^+-ion. The large cationic size of Na^+-ion always tries to remain in the octahedral and prismatic void with a 6-coordination number rather than in the tetrahedral void [19,20].

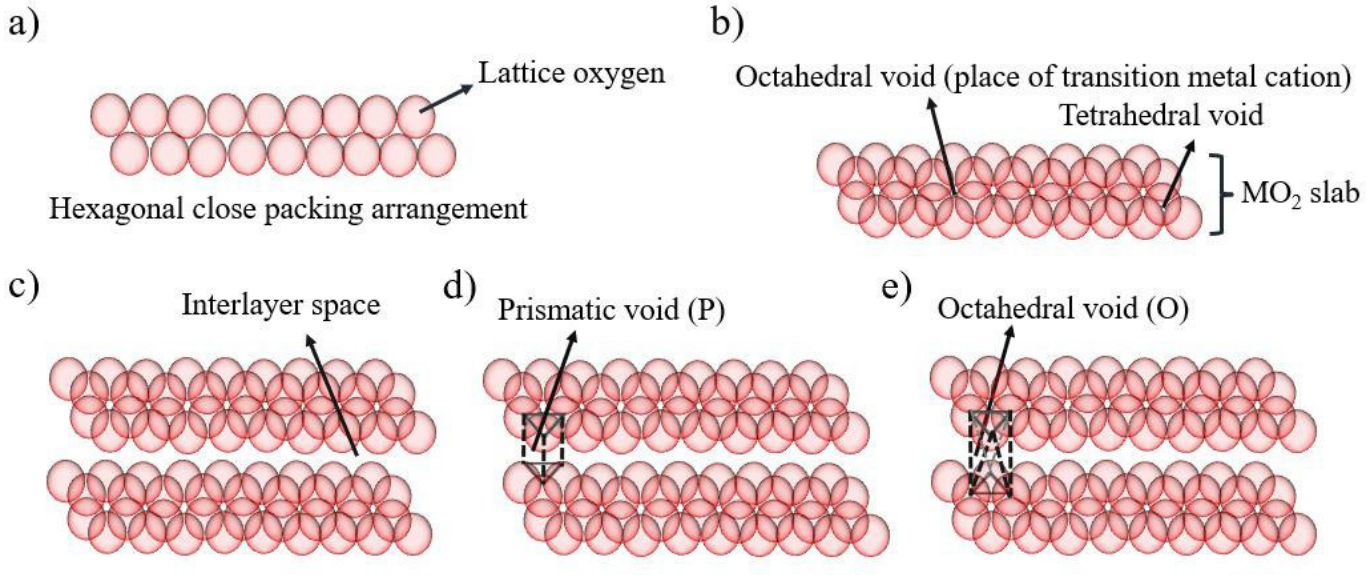


Figure 2. (a) Lattice oxygen packing, (b) void formation, (c) parallel arrangement of MO_2 slabs, (d) prismatic and (e) octahedral void formation respectively.

The structure is important in reaching electrons' high ionic and eltectronic conductivity. P2-type material offers a lower energy conduction pathway than O2-type material for Na^+-ion mobility. Na^+-ions can be moved from one octahedral site to an adjacent site in an O2-type phase occupying a tetrahedral site as shown in **Figure 3 (a)**, this entails passing through a common triangular face that stands between the octahedral-tetrahedral site, which results in a comparatively high activation barrier. The intermediate state's energy is increased by the potent coulombic repulsions between the transition metal ions (cation) in the MO_2 layers and the ions in the tetrahedral locations due to the closely packed system [21]. On the other hand, Na^+-ions in P2-type layered phases are dispersed over several trigonal prisms i.e. the Na sublattice is only partially filled, sharing their rectangular faces and offering extensive pathways and wider passage for the transport of Na^+-ions.

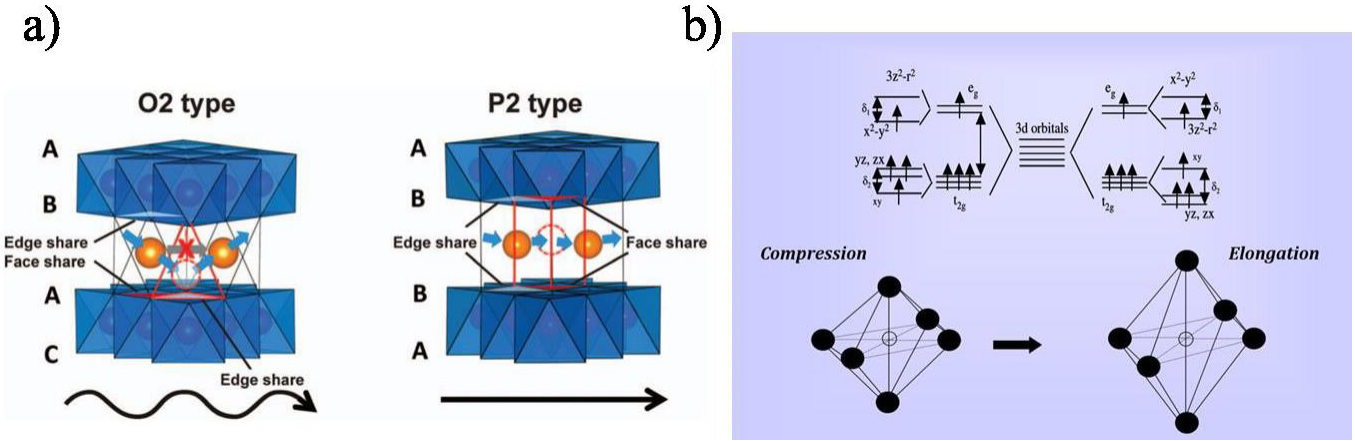


Figure 3. a) Na^+-ion conduction pathways in layered oxide O2-type and P2-type material [22], b) a schematic view of Jahn-Teller active species (Mn^{3+}ion)

Despite these advantages of P2-type layered cathode material. it undergoes poor reversibility and severe capacity loss due to the structure's instability. Various factors affect the structural integrity; phase transition is common in P2-type layered oxide material. In the high potential window while charging, Na^+-ions are extracted from the interlayer

spacing between the MO_2 slabs and a few ions maintain the initial structure. When the maximum number of Na^+ ions are extracted, the O^{2-} ions, positioned directly above one another, begin to repel each other. This repulsion is alleviated by the sliding of the oxygen layer, resulting in the formation of the more energetically stable O2-type phase. Consequently, Na^+-ion vacancies are less stable in the P2-type phase [23].

Another one is the presence of the Jahn-Teller (JT) active species in layered systems, Mn-based NaBs are low-cost, sustainable, and environmentally friendly energy storage technologies. Layered P2-type Na_XMnO_2 is more commonly investigated than the other [19]. The P2-type Na_XMnO_2 crystallizes in the two-phase tunnel-like structure with low sodium content (e.g. $Na_{0.2}MnO_2$, $Na_{0.4}MnO_2$, $Na_{0.44}MnO_2$), and layered structure with MO_2 slabs at high sodium content (e.g. $Na_{0.7}MnO_2$, $NaMnO_2$) [19].

In P2-type Na_XMnO_2, Mn^{3+} with electronic configuration t_{2g}^3 e_g^1 is JT active. In the MO_2 slab, the JT active species disturb the unit cell's symmetrical arrangement due to the elongation and compression of the bonds [24] shown in **Figure 3 (b)**. Na^+-ion conduction is affected by the activation energy barrier for Na^+-ion migration between neighboring sites when vacancy ordering or JT active cations (like Mn^{3+}) are present [25]. The strongly disfavoured unoccupied prismatic sites in a partially charged state and sudden change to an O2-like structure, as was previously described, can be challenging to create a stable P2 structure in practice [23].

The distortion highly depends on the synthesis conditions, low-temperature condition with a highly oxidizing environment stabilizes the Mn^{4+} state which reduces the distortion in the P2-type material. A study of the tunnel-like Na_XMnO_2 (x = 0.19–0.44) cathode material, reveals the anisotropic expansion during cycling is due to the presence of mixed valance Mn^{3+}/Mn^{4+} leads to the poor cycling performance of P2-type Na_XMnO_2. Initially, the structure of Na_XMnO_2 as the sodium content x increases from 0.22 to 0.66, the material's structure expands along the b-axis. Additionally, further expansion occurs along the a- and c-axes as x increases from 0.44 to 0.66. This anisotropic expansion behavior is crucial for understanding the material's performance in NaBs. The presence of JT Mn^{3+} species at different lattice positions leads to anisotropic changes in the lattice parameter along the a-, b-, and c-axis, resulting in the loss of capacity [26]. Apart from this, irreversible anionic redox causes severe capacity decay and disturbs the structural integrity. Generally, it occurs in the high potential window (> 4.3 V vs Na^+/Na), and forms unstable recombination of over-oxidized lattice oxygen (O^{2-}) further releases as O_2 gas which leads to the structural transformation from layered to spinel [27–29]. Recent studies indicate that the O_2 molecule can be trapped in the bulk [30–32]. O_2 gas evolution occurs at the surface of the particle and enters into the bulk of the material which generates vacancies and causes capacity degradation [33,34].

The oxygen release in P2-type Na_xMnO_2 is still unclear. Enhancing the performance of cathode materials is a critical focus in the expansion of high-efficiency NaBs. Several strategies are employed to achieve this, aiming to address challenges such as low energy density, poor cycling stability, and limited rate capability. One key practice is the optimization of cathode material composition. Researchers are investigating doping strategies, where small amounts of specific elements are introduced to stabilize the cathode structure, improve electronic conductivity, and facilitate sodium ion diffusion.

3. Strategies to address the issues

3.1 To design a high-capacity cathode

The P2-type phase is only stable with a limited amount of sodium i.e. Na_X where $x \leq 2/3$ [35]. It is impossible to increase the Na amount up to 0.9 with a stable P2-phase [36,37]. The as-synthesized P2-type phases can have their Na content raised by transition metal substitution, as **Figure 4** illustrates. The MnO_2 layers have been doped to increase the P2-type Na_XMnO_2's maximum capacity. Mn can be partially substituted for Ni, Li, or both to stabilize P2 structures with a Na concentration as high as 0.85. The maximum cutoff

voltage is restricted to approximately 4.2 V to avoid any structural alterations that would impact the reversible reinsertion of Na^+-ion into the structure after discharge. Therefore, materials in which part of the Mn has been replaced by Ni and Li have only moderate reversible capacities (63 to 140 mAh g^{-1}) [38–40].

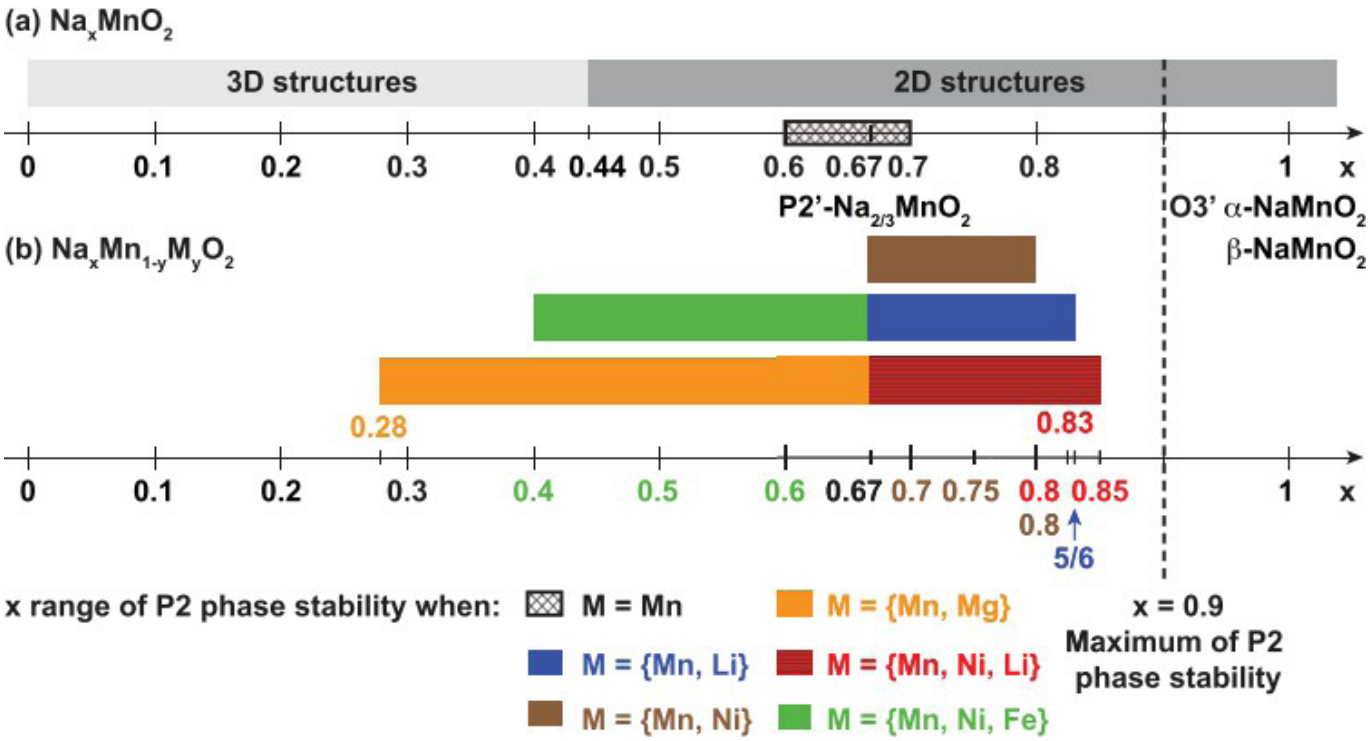


Figure 4. (a) Range of sodium content [77] in P2-Na_xMnO_2 compound observed for 3D and 2D structural stability [41,42], (b) doping of various elements on the Mn site to stabilize the P2-phase of the Na_xMnO_2 compound M = {Mn, Ni}[43]{Mn, Li} [35] {Mn, Mg}[44] {Mn, Ni, Li}[45–47] {Mn, Ni, Fe} [48].

3.2 To raise the potential window of P2-type cathode material

In the context of A_xMO_2 (A=Li, Na) materials, the electrochemical performance is highly influenced by substituting transition metals. This substitution can adjust key features, such as the value of voltage wherein the system material (de)/intercalates Li^+/Na^+ ions. For instance, P2-Na_xMnO_2 has been observed to operate within a narrow voltage range of approximately 2.8 V vs. Na^+/Na, but it offers a high capacity between 175 mAh g^{-1} and 190 mAh g^{-1} [49,50]. However, research into Fe-based systems, such as O3-$NaFeO_2$, which exhibits a higher redox potential of around 3.3 V vs. Na^+/Na, has led to new developments [51]. Yabuuchi and colleagues explored the stabilization of the P2-phase by partially substituting Mn^{3+} with Fe^{3+} in P2-$Na_xFe1/2Mn1/2O2$. Their findings demonstrated that both Mn^{3+}/Mn^{4+} and Fe^{3+}/Fe^{4+} redox couples were active, resulting in a reversible capacity of 190 mAh g^{-1} when cycled between 1.5 and 4.2 V at a 12 mA g^{-1} rate. However, contrary to expectations, this Fe/Mn bimetallic oxide did not demonstrate an increase in average working voltage, remaining around 2.75 V, similar to P2-Na_xMnO_2 [9]. Furthermore, Lu and Dahn synthesized the P2-$Na_{2/3}Ni_{1/3}Mn_{2/3}O_2$ electrode to investigate the influence of Ni replacement within the electrochemical characteristics of P2-Na_xMnO_2, adding another layer of complexity and potential for performance enhancement in these materials [52].

3.3 To suppress P2-O2 phase transition in P2-type cathode m15

single-phase behavior in P2-type layered oxides during cycling is crucial for ensuring their electrochemical stability and longevity. Investigations are concentrated on fine-tuning the composition and structure of these materials to avoid undesirable cation-ordering transitions and to enhance their performance in NaBs. The stability of P2 phases is essential for achieving high-rate performance in Na cells. However, prolonged cycling can lead to side reactions that compromise the P2 phase, resulting in increasedoverpotential and capacity loss, often due to low reversible capacity and poor capacity retention. To address these challenges, careful selection of synthetic conditions such as the choice of precursors, preparation temperature, and cooling method (slow cooling vs. quenching) is critical in achieving single-phase behavior. Additionally, composition plays a key role in preserving the stability of the P2 structure during cycling. A common approach to restrict the oxygen layer from sliding after Na deintercalation and to extend the stability range of the P2 structure over varying Na content is the addition of dopants into the MO_2 layer. For instance, as presented in **Figure 4**, substitutedNa_xMnO_2 phases benefit from such doping. Specifically, Li-doped P2-Na_xMO_2 (M = Ni, Mn) compounds have been shown to remain stable up to a potential of 4.2 V, which corresponds to a Na amount of 0.35 [40,47]. Despite these advancements, the exact content of Na required to remain in the Na_xMO_2 structure to resist the structural changes at high voltage continues to be a topic of ongoing research and debate [46]. The balance between stability and performance remains a key area of focus for optimizing these materials for practical applications.

3.4 To ensure structural stability by diluting the Jahn-Teller species

In P2-type intercalation electrode materials, structural stability is crucial for ensuring reversible electrochemical behavior and achieving a long cycle life. One of the significant challenges in maintaining structural stability is the presence of Jahn-Teller (JT) active Mn^{3+} species, which can induce distortions during cycling. These distortions create large stresses on the lattice parameters, leading to the accumulation of extended defects and even amorphization, particularly after prolonged cycling [53]. To mitigate the effects of JT distortions, the dilution of Mn^{3+} is an effective strategy. By substituting Mn^{3+} with other elements, the influence of JT active species can be reduced. Paulsen and Dahn demonstrated that the monoclinic distortion observed in β-$Na_{0.7}MnO_2$ transitions to an orthorhombic structure when weakly substituted with elements like Co, Li, or Ni in $Na_{2/3}Mn_{1-x}M_xO_2$. In heavily substituted samples, an ideal P2 structure is observed, indicating that substitution plays a key role in stabilizing the material [54]. Substituting Mn^{3+} with lower valence elements not only decreases the amount of Mn ions in the material but also increases the average Mn oxidation state from +3 to +4. This change in oxidation state reduces the extent of JT distortions, contributing to a more stable structure during cycling. Furthermore, doping can create a more flexible structure with minimal volume changes during cycling, enhancing the material's overall stability. The insertion of low valence spectator ions, such as Li^+, can also effectively stabilize the P2 phase across a wide voltage range. This approach helps maintain structural integrity, even under high-voltage conditions, making the material more suitable for long-term cycling in battery applications.

Doping elements into cathode materials is a crucial strategy for improving the performance of NaBs. This technique involves adding specific elements to the cathode structure to enhance its electrochemical properties, such as stability, capacity, and conductivity. By selecting appropriate dopants, researchers can address common challenges associated with Na-ion battery cathodes, like low energy density and poor cycling stability. For instance, doping with transition metals such as Mg, Zn, or Al can help stabilize the crystal structure of layered oxide cathodes, reducing structural degradation during charge-discharge cycles and thereby extending the battery's lifespan. Additionally, dopants can improve the electronic and ionic conductivity of the cathode material, leading to faster sodium ion diffusion and better rate

capability. Some dopants also help in mitigating the volume changes that occur during cycling, which can otherwise lead to capacity fading. Overall, element doping is a versatile and effective approach to developing high-performance cathodes, which are essential for advancing the efficiency and reliability of NaBs. Hence, doping opens the way to introduce HCE in the material, which offers a more flexible structure with low volumetric expansion and contraction, it helps to reduce the P2-O2 phase transition upon cycling in the high voltage range. By introducing various dopant elements such as active, inactive, and high valent, one can stabilize the P2-type phase of the material. Doping also helps to reduce the JT active species, lowering the energy barrier for the Na^+-ion conduction during charging and discharging. Incorporating doping elements into cathode materials can increase the CE, thereby enhancing the stability and electrochemical performance of NaBs.

2. Concept of configurational entropy

Based on thermodynamics, entropy is the microstructure combination that constitutes a specific macroscopic state. The concept itself originated from the thought experiment and approach of postulates. The thought experiment consists of a macroscopic closed composite system with total volume (V), and internal energy (U), composed of several particles (N) separated by an impermeable membrane that divides the system into two regions, in which system 1 is defined as (V_1, U_1, N_1) with entropy S_1 and system 2 described as (V_2, U_2, N_2) with entropy S_2. If the membrane is permeable the two systems try to reach the equilibrium as shown in **Figure 5 (a, b)**. After some time, at equilibrium state particles will be randomly arranged, and the entropy of the system will become $S = S_1 + S_2$. N_1 (number of particles of system 1) and N_2 (number of particles of system 2) can access a larger volume (V) to spread randomly throughout the system. There exists a function S (entropy) in the absence of the internal constraints (without impermeable membrane) which maximizes S (entropy) at the equilibrium state and this is known as the entropy of the system (entropy is additive in nature) [55].

A macroscopic system as discussed above can be thought of in another way, with a permeable membrane, N_1 and N_2 can occupy the maximum number of possible microstates available in volume (V). The probability of occupying each available state in the system gives the number of configurations and is calculated by the formula given below shown in **Figure 5 (c, d)**.

$$\Omega = N! / N_1! N_2!$$

After some time, the system reaches equilibrium, with the maximum possible configurations for N_1 and N_2 particles. This builds the connection between the macroscopic system and a number of available microstates (microscopic system) given by the Boltzmann relation stated as below [55].

$$\Delta S_{conf} = \kappa \ln \Omega \text{ (fundamental postulate)}$$

Where κ is the Boltzmann constant and Ω is the number of available microstates for the particles in the system.

For a 2-component system, with n_1 and n_2 a lattice, where total number of molecules are $n = n_1 + n_2$

Therefore, the number of lattice sites can be calculated by the permutation and combination for the given system and is provided by the formula ($\Omega = n! / n_1! n_2!$). By applying Stirling's approximation for the factorial of a large integer CE can be given as follows;

$$\Delta S_{conf} = \kappa \ln \Omega$$

$$\Delta S_{conf} = - R [n_1/n \, ln \, n_1/n + n_2/n \, ln \, n_2/n] \; x_1 = n_1/n; \; x_2 = n_2/n$$

$$\Delta S_{conf} = - R [x_1 \, ln \, x_1 + x_2 \, ln \, x_2]$$

The CE change per mole for n components with x_i mole fraction when forming a solid solution is given as [56].

$$\Delta S_{conf} = - R [\sum_{i=1}^{n} x_i \, ln \, x_i]$$

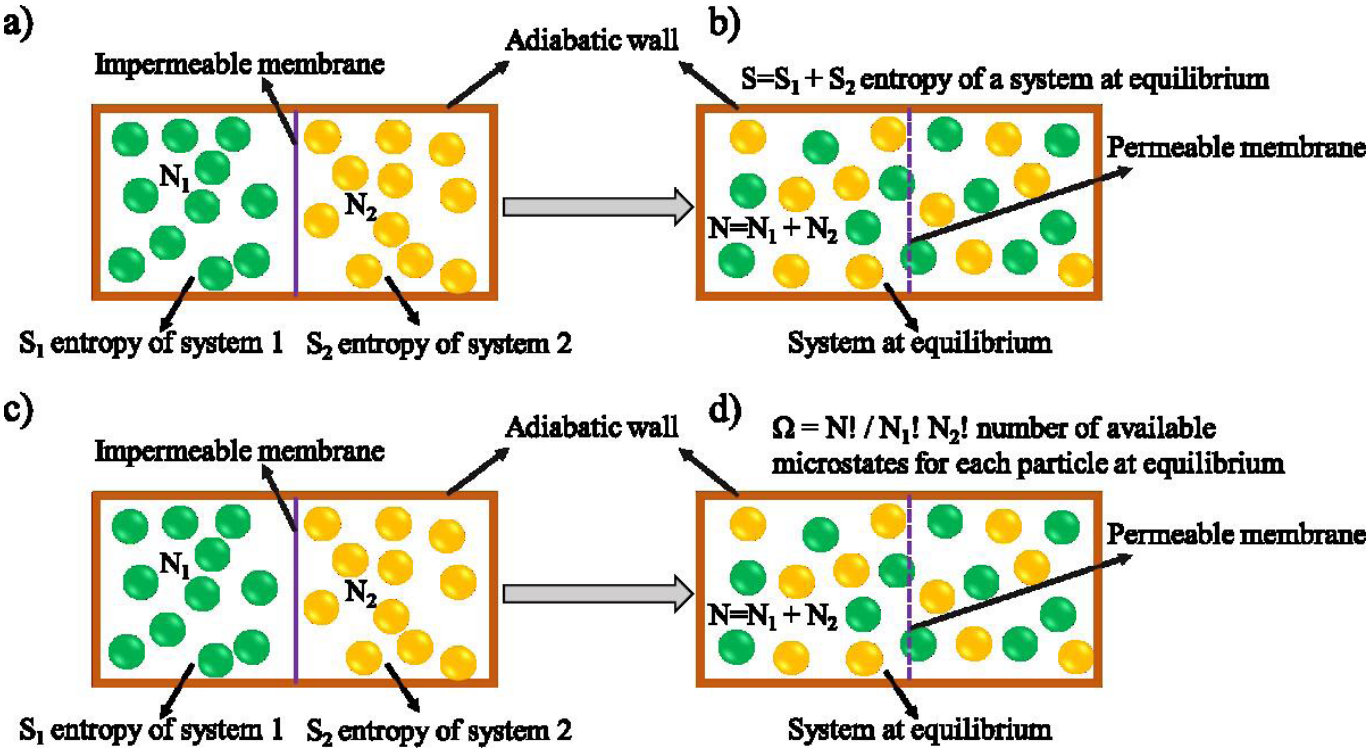


Figure 5. (a, b) Entropy of the system at equilibrium based on the entropy postulate, (c, d) number of configurations at equilibrium [55].

For a 2-component system, with n1 and n2 a lattice, where total number of molecules are **n = n1 + n2**

Therefore, the number of lattice sites can be calculated by the permutation and combination for the given system and is provided by the formula **(Ω = n! / n1! n2!).** By applying Stirling's approximation for the factorial of a large integer CE can be given as follows;

ΔSconf = κ ln Ω

ΔSconf = - R [n1/n *ln* n1/n + n2/n *ln* n2/n] x1 = n1/n; x2 = n2/n

ΔSconf = - R [x1 *ln* x1 + x2 *ln* x2]

The CE change per mole for n components with x_i mole fraction when forming a solid solution is given as [56].

ΔSconf = - R [$\sum_{i=1}^{n}$ xi *ln* xi]

4.1 Definition

The investigation of unexplored areas in the field of alloying engineering gives birth to HEMs [57]. The evolution of HEMs was initiated by conventional alloys; pure single crystalline material consists of a single element placed on a fixed lattice position. The demand for more advanced materials was fulfilled by the binary and ternary compounds, in which two or three elements were mixed in small amounts with a non-equimolar ratio to substitute the pure elements lattice position and known as conventional alloys that may or may not be crystallized in a single phase. In 2004, researchers explored the equimolar region with five or more than five elements where the position of the component/element is not fixed and it arranges itself randomly throughout the lattice, surprisingly found that it crystallizes in a single phase known as high entropy alloys [58,59]. Recently, in 2018 the focus has been on the non-equimolar composition around the center [60] of the hyperdimensional compositional diagram as shown in **Figure 6 (a)**, which was explored intensively and again represents the random arrangement of elements in the system leads to an increase in the entropy known as

complex concentrated alloys (CCAs) [61].

The entropy of mixing in a solid solution refers to the increase in disorder when different types of atoms or species mix in a crystalline solid. This entropy is composed of several contributions, each related to different types of disorder and energy states within the material. This is the most significant contributor to the entropy of mixing in a solid solution. It arises from the random arrangement of different atoms (or ions) on a lattice site. For an ideal solid solution, CE $\Delta S_{conf} = -R\left[\sum_{i=1}^{n} x_i \ln x_i\right]$. The more randomly distributed the different atoms are, the greater the CE. Vibrational entropy arises from the atomic vibrations within the solid. Different atoms or ions have distinct masses and bonding strengths, which influence the vibrational modes of the solid. When atoms of different types mix, the vibrational frequencies shift, which can either increase or decrease the vibrational entropy. This effect is more pronounced in alloys or systems where there is a significant difference in atomic mass between the components. This contribution is relevant in materials where the atoms have magnetic moments. Magnetic dipole entropy arises from the disorder in the orientations of magnetic moments (spins) in the material. For materials that exhibit magnetic ordering, such as ferromagnets or antiferromagnets, the mixing of different atoms with varying magnetic properties can lead to changes in the magnetic dipole entropy. The degree of disorder in the magnetic system, particularly at temperatures near or above the Curie or Néel temperature, adds to the overall entropy. This is often referred to as residual entropy, which occurs when the system remains disordered even at very low temperatures. This type of entropy is present in systems that have more than one equivalent ground state, such as certain frustrated magnetic materials or systems with random occupancy of certain lattice sites (without long-range order). Residual entropy can arise when the system does not achieve perfect order even as temperature approaches absolute zero. Overall, the entropy of mixing in a solid solution is a combination of various forms of disorder, CE relates to the atomic arrangement, vibrational entropy comes from atomic vibrations, and magnetic dipole entropy is due to the disorder in magnetic moments. Random (residual) entropy arises from the inherent disorder at low temperatures. Together, these components contribute to the total entropy of the solid solution, influencing its stability and behavior, especially in thermodynamic processes like phase transitions [62].

CE is dominant in all, which usually represents the entropy of mixing and depends on the elemental proportion [63]. Hence, an efficient way to reach the HCE is to introduce various elements in a specific system. The HCE materials are commonly identified based on the composition of the system and the entropy calculation. The definition of HCE is still unclear and can be divided into two, 1st is based on the composition which describes a system with five or more elements in the equimolar ratio (range of elements 5 to 35%) [59], 2nd is based on entropy which defines the system with HCE i.e. the entropy must be larger than 1.5R, without any restriction on the elemental composition [64]. The maximum S_{conf} is 1.61R, which may be obtained in a system with five cations at equiatomic proportions. Materials with $S_{conf} < 1R$ are classified as "low entropy," those with $1.5R > S_{conf} \geq 1R$ are classified as "medium entropy," and materials with $S_{conf} \geq 1.5R$ are classified as "high entropy" systems. Thus, to create materials with significant CE, the systems intentionally integrate a major proportion of numerous elements in about equal proportions. This method differs from traditional doping procedures as it extends beyond the trace amount of doping and is typified by a more broad and well-balanced compositional range of elemental variety [65]. A system with five or more elements tends to form a single-phase solid solution with HCEs but this is not always the case [66]. To understand how entropy affects a compound's phase stability, consider the Gibbs free energy of mixing ΔG_{mix} as given by the below equation;

$$\Delta G_{mix} = \Delta H_{mix} - T\Delta S_{mix}$$

Where ΔS_{mix} denotes the mixing entropy in the above equation, the mixing enthalpy by ΔH_{mix}, and the mixing CE by ΔS_{conf}, which usually dominates in ΔS_{mix}. The absolute temperature is indicated by T.

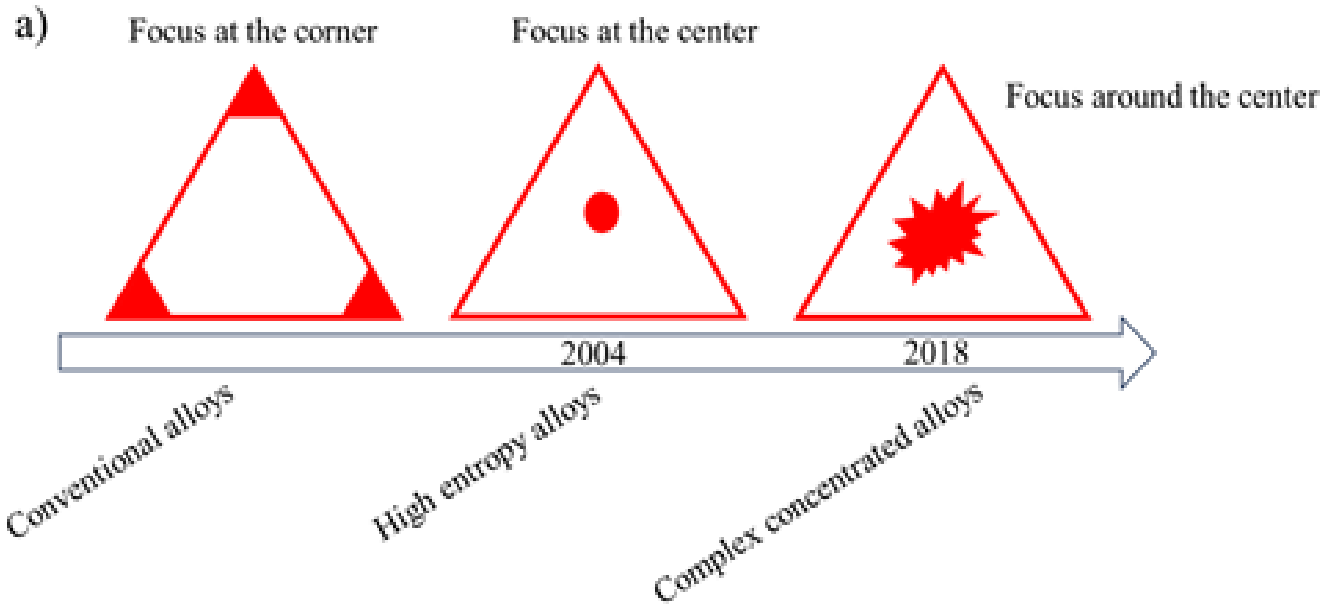


Figure 6. (a) Evolution of material innovation and the birth of high-entropy material

In the formation of HCEs and to stabilize the phase of the material there is always a competition between enthalpy and entropy. The enthalpy of a multi-component system varies significantly since the nature of the constituent elements in a solid solution plays a critical role in determining the resulting phase under near-equilibrium conditions. These elements influence various factors, including atomic size, electronegativity, crystal structure, and bonding characteristics, which in turn dictate phase stability and transitions. If the elemental composition has highly positive values of negative ΔH_{mix} (indicative of repulsive forces), this can lead to immiscibility and phase segregation. Conversely, highly negative ΔH_{mix} values (indicative of attractive forces) promote structural ordering, such as the formation of intermetallic compounds. If all ΔH_{mix} pairs in the multi-element composition are near-zero, indicating minimal attraction or repulsion between elements, the entropic term becomes dominant. This entropic dominance promotes homogeneous random elemental mixing, leading to HCE. However, natural single-phase mixing, especially in solid solutions, is indeed challenging and relatively rare due to the inherent complexities of atomic interactions and structural stability. Several factors contribute to this difficulty, making it hard to achieve and maintain a homogeneous single-phase structure in nature or even in controlled environments due to the significant physicochemical differences among different elements, which result in a wide range of ΔH_{mix} values [67,68]. For metal oxides, each cation is surrounded by anions (i.e. oxygen lattice), which have the same environment. This leads to $\Delta H_{mix} = 0$ and leaves only the entropy term in the Gibbs free energy equation, hence phase stabilization is affected by the entropy of mixing [18].

$$\Delta G_{mix} = \Delta H_{mix} - RT \sum_{i=1}^{n} x_i \ln x_i$$

It is possible to reach one phase in many cases when $S_{conf} \geq 1.5$ R. In these situations, entropy stabilization is established by the dominance of the $T\Delta S_{mix}$ term in the free energy landscape, which surpasses ΔH_{mix} and results in a negative overall ΔG_{mix} [69]. It's crucial to remember that entropy and temperature are strongly related, and synthesis at higher temperatures typically encourages the creation of single-phased systems with higher CEs.

4.2 How to achieve high configurational entropy?

Generally, it was observed that the existence of numerous elements in the system will give the maximum CE. However, this is not always feasible. The CE of the system is dependent on the number and the mole fraction of the elements in the system. For a two-component system (e.g., system A and system B maximization of CE takes place at XA=XB=0.5, it was calculated mathematically by using the formula which indicates that the maximum possible achievable entropy in two components is 5.76 J/K mol as shown in **Table 1 (a)**. This suggests that the multi-component system in an equimolar ratio always maximizes the CE [56]. In addition, the CE can be maximized by increasing the number of elements. Where we observe that the HCE will be achieved with five or more than five elemental compositions in the given system as shown in **Table 1 (b)**.

Table 1. (a) Entropy calculation for a 2-component system, (b) entropy calculation with increasing number of elements

a)

x_A	x_B	$\Delta S_{conf} = -R [x_A \ln x_A + x_B \ln x_B]$
1	0	0
0.9	0.1	2.7
0.8	0.2	4.16
0.7	0.3	5.07
0.6	0.4	5.59
0.5	0.5	5.76
0.4	0.6	5.59

b)

No. of components	Equimolar ratio	$S_{conf} = -R [\sum x_A \ln x_A]$
1	1	0
2	0.50	5.76
3	0.33	9.220
4	0.25	11.64
5	0.20	13.38

4.3. Recent progress of P2-type material towards high configurational entropy

Recent advancements in P2-type materials have shown significant promise for improving the performance of NaBs. These materials, characterized by their layered structure, offer high Na-ion mobility and structural stability, making them ideal candidates for cathodes in NaBs. Research has focused on optimizing their composition, such as through element doping to enhance their electrochemical properties. These improvements have led to better capacity retention, increased energy density, and prolonged cycle life, positioning P2-type materials as a leading option in the development of next-generation NaBs. Research on phase shifts in layered materials during electrochemical cycling has been a fascinating topic for a long time. The P2 structure, while interesting, faces some challenges. Na^+ vacancy ordering and troublesome P2-O2 phase transitions can negatively affect material capacity & cycle performance. Manganese (Mn) is very important, it's a key part of layered oxides and also plays a crucial role in P2-type materials. At higher potentials (more than 2.0 V), Mn^{+4} ions help keep the structure stable during discharge (when it gets sodiated). But as the electrode discharges below 2.0 V, those Mn^{4+} ions get reduced to Mn^{3+}. This change increases the concentration of JT-active Mn^{3+}, which plays a major role in degrading electrochemical characteristics. This can lead to lattice deformation, active material loss, and even create new phases. To tackle these issues, one of the best strategies is to reduce unwanted phase transitions & control Mn loss during cycling.

In 2022, Wang et al. synthesized three different P2-type layered oxide cathode materials using a solid-state method: $Na^{0.67}(Mn^{0.55}Ni0.^{21}Co^{0.24})O^2$, $Na^{0.67}(Mn^{0.45}Ni^{0.18}Co^{0.24}Ti^{0.1}Mg^{0.03})O^2$, and $Na^{0.67}(Mn^{0.45}Ni^{0.18}Co^{0.18}Ti^{0.1}Mg^{0.03}A^{l0.04}Fe^{0.02})O^2$. Named as 3, 5, and 7 NTMO2 and according to their entropy properties, low (0.99 R), medium (1.34 R), and high (1.52 R) respectively [70]. The material with the highest entropy showed amazing reversibility with less Mn depletion and structural deterioration within the voltage ranges of 1.5–4.6 V and 2.6–4.6 V, while medium & low entropy materials experienced moderate to rapid capacity loss respectively.

It turns out that improving CE is a smart way to avert phase transition while boosting structural stability. In 2023, Dreyer et al. used sonic emission to check how an increase in CE affected phase-transition properties in those high entropy oxides we talked about 3, 5 & 7 NTMO2. The distinct sound signatures linked to fracture creation were quite noticeable [71]. Shen et al. shared details about a P2-type cathode ($Na_{0.80}Li_{0.08}Ni_{0.22}Mn_{0.67}O_2$) aimed at raising the cut-off voltage to start anionic redox [72]. Similarly, Jin et al. crafted a new $Na_{0.75}Ca_{0.04}[Li_{0.1}Ni_{0.2}Mn_{0.67}]O_2$ P2-cathode helping with anionic redox-related capacity loss using Manganese (+3/+4) redox complementary mechanism. At a remarkable rate of 5C over two hundred cycles, this cathode held on strong with an impressive retention of around 95% [73]. The P2-$Na^{o}.^{62}Mn^{o}.^{67}Ni^{0}.^{23}Cu^{o}.^{05}Mg^{o}.^{09}$–²yTiyO² showed better Na^{+} diffusion thanks to its higher fraction regarding facets {010} along with improved entropy, this was highlighted by Fu et al. The kinetics of anionic redox reactions were also improved due to features from the crystal structure in the P2 phase [74]. Also noteworthy is that the Na^{+} diffusion coefficient related to various cathode materials such as CuMgTi-571 and NaMNO2 during Na (de) intercalation looks promising. Plus, managing energy through entropy fluctuation can contribute positively to performance. For example, $Na^{o}.^{62}Mn^{o}.^{67}Ni^{o}.^{23}Cu^{o}.^{05}Mg^{o}.^{07}Ti^{o}.^{01}O^{2}$ showed an extraordinary capacity of about 82 mAh g^{-1} at a rate of 1200 mA g^{-1}. Ma et al. developed another cathode called P2-$Na^{o}.^{667}Mn^{o}.^{667}Ni^{o}.^{167}Co^{o}.^{117}Ti^{o}.^{01}Mg^{o}.^{01}Cu^{o}.^{01}Mo^{o}.^{01}Nb^{o}.^{01}O^{2}$ (HCE-NMNC). In this case, five cations share equal proportions at TM sites [75]. High entropy doping helps minimize strain change by widening voltage ranges for the highly reversible P2 phase. The HCE-NMNC managed a capacity of 111 mAh g^{-1} at 5C which was steady over one hundred cycles at 1C (130 mAh g^{-1}). The reversible oxygen redox process from its lattice site during cycling, and the charge compensation by metals like Ni, Co & Mn contributed to this high potential capacity.

Recently many reports about medium entropy oxides (MEOs) have come out. Yan et al., back in 2021 published their first report using MEOs in NaBs [76]. They developed two types of P2-compositions using solid-state methods: $Na_{2/3}Ni_{1/3}Mn_{1/3}Fe_{1/3-x}Al_xO_2$ (NaNMF) and $Na_{2/3}Ni_{1/3}Mn_{1/3}Fe_{1/3-x}Al_xO_2$ (NaNMFA) featuring three & four cation replacements respectively. The four-cation system NaNMFA showed better cycle stability between two volts & four point two volts compared to the three-cation system NaNMF with around 125.6 mAh g^{-1} reversibility. Research suggested that HCE led to smoother charge-discharge curves which also helped inhibit structural transitions raised due to damaging Mn^{3+}, preserving crystal structure integrity. Wang et al. worked on HCE-(P2-$Na_{0.65}Mn_{0.65}Cu_{0.2}Li_{0.06}Mg_{0.015}Ti_{0.015}Al_{0.015}Zr_{0.015}Y_{0.015}La_{0.015}O_2$) showing potential against those irreversible phase transitions while minimizing significant volume changes when charging or discharging batteries [77]. They reported on another cathode via Liu et al. called P2-type $Na_{0.85}Li_{0.12}Ni_{0.198}Be_{0.011}Mg_{0.011}Mn_{0.66}O_2$ designed with a lower Mn^{3+}/Mn^{4+} ratio too. In this case, widening interlayer distances ensures amazing rate performance. The two published patents for positive electrode materials concerning P2-HCE oxide recently, the first patent on P2-$Na_{0.67}Ni_{0.18y}Cu_{0.1}Zn_{0.05}Fe_xMn_{0.67-x+y}O_2$ stated a capacity around 105.3 mAh g^{-1} at 1C with retention of nearly 93%. The second patent discussed P2-$Na^{o}.^{75}Mn^{o}.^{5625}Ni^{o}.^{25}Cu^{o}.^{0625}Mg^{o}.^{0625}Ti^{0}.^{0625}O^{2}$ showcasing 98%. It shows incredible retention after 100 cycles starting from approximately 108 mAh g^{-1} around 120 mA g^{-1} (2–4.3 V) [77].

5. Discussion and future direction for the development of cathode

The dependence on energy storage devices especially in developing next-generation cathode material for NaBs, performance enhancement like energy density, reversibility, structural stability, and phase transition is crucial. Traditional aspects of cathode modification like elemental doping are still insufficient to achieve the aim of superior-performance batteries. Fortunately, the advancement of HCEs aims to preserve the single-phase with a highly flexible structure and diverse material

compositions and architectures, unlocking new pathways to enhance battery materials development. Research into HCE materials for batteries is still in the early stages, but the potential for these materials to revolutionize battery technology is significant. As our understanding of HCE behavior in electrochemical systems deepens, we can expect to see more HCE material-based components in commercial batteries, leading to higher performance and more durable energy storage solutions. Hence, HCE can indeed be a promising strategy for developing cathode materials for NaBs. By incorporating multiple cations in a single lattice (often five or more), the CE of the system is increased. This entropy can stabilize the crystal structure even at room temperature, preventing phase separation and ensuring a more stable cathode material over multiple charge/discharge cycles. In NaBs, cathodes face challenges like phase transitions and structural degradation during cycling. HCE can help mitigate these issues by stabilizing different phases that might otherwise be unstable. This leads to improved cycle life and performance. The presence of multiple different metal ions can lead to synergistic effects, improving electronic conductivity, ionic conductivity, and overall electrochemical performance. This is particularly important for NaBs, where finding suitable cathode materials has been more challenging than for their Li-ion counterparts. HCE materials offer the flexibility to fine-tune the composition by adjusting the ratio of different elements. This tunability allows researchers to optimize properties such as capacity, voltage, and stability for specific applications. In summary, HCE offers a pathway to develop a P2-type layered oxide cathode for NaBs with enhanced stability, good performance, and sustainability.

Acknowledgment

Amrapali appreciates the funding support from STARS ID-2023- and 0738, Code: RD/0123-STARS00-005, Grant:10018185. Also, acknowledges the Department of Energy Science and Engineering of the Indian Institute of Technology, Bombay, for offering the Institute Teaching Assistant (TA-category) Research Fellowship.

Conflict of interest

The author declares no conflict of interest.

References:

[1] E. Goikolea, V. Palomares, S. Wang, I.R. de Larramendi, X. Guo, G. Wang, T. Rojo, Na-Ion Batteries–Approaching Old and New Challenges, Adv Energy Mater 10 (2020). https://doi.org/10.1002/aenm.202002055.

[2] J.F. Peters, M. Baumann, J.R. Binder, M. Weil, On the environmental competitiveness of sodium-ion batteries under a full life cycle perspective-a cell-chemistry specific modelling approach, Sustain Energy Fuels 5 (2021) 6414–6429. https://doi.org/10.1039/d1se01292d.

[3] P.K. Nayak, L. Yang, W. Brehm, P. Adelhelm, Von Lithium- zu Natriumionenbatterien: Vorteile, Herausforderungen und Überraschendes, Angewandte Chemie 130 (2018) 106–126. https://doi.org/10.1002/ange.201703772.

[4] X. Xiang, K. Zhang, J. Chen, Recent advances and prospects of cathode materials for sodium-ion batteries, Advanced Materials 27 (2015) 5343–5364. https://doi.org/10.1002/adma.201501527.

[5] M. Dahbi, N. Yabuuchi, K. Kubota, K. Tokiwa, S. Komaba, Negative electrodes for Na-ion batteries, Physical Chemistry Chemical Physics 16 (2014) 15007–15028. https://doi.org/10.1039/c4cp00826j.

[6] Y. Kim, Y. Kim, A. Choi, S. Woo, D. Mok, N.S. Choi, Y.S. Jung, J.H. Ryu, S.M. Oh, K.T. Lee, Tin phosphide as a promising anode material for Na-ion batteries, Advanced Materials 26 (2014) 4139–4144. https://doi.org/10.1002/adma.201305638.

[7] J. Qian, X. Wu, Y. Cao, X. Ai, H. Yang, High capacity and rate capability of amorphous phosphorus for sodium ion batteries, Angewandte Chemie - International Edition 52 (2013) 4633–4636. https://doi.org/10.1002/anie.201209689.

[8] S. Guo, H. Yu, Z. Jian, P. Liu, Y. Zhu, X. Guo, M.

Chen, M. Ishida, H. Zhou, A high-capacity, low-cost layered sodium manganese oxide material as cathode for sodium-ion batteries, ChemSusChem 7 (2014) 2115–2119. https://doi.org/10.1002/cssc.201402138.

[9] N. Yabuuchi, M. Kajiyama, J. Iwatate, H. Nishikawa, S. Hitomi, R. Okuyama, R. Usui, Y. Yamada, S. Komaba, P2-type Nax [Fe1/2 Mn1/2[O2 made from earth-abundant elements for rechargeable NaÂ batteries, Nat Mater 11 (2012) 512–517. https://doi.org/10.1038/nmat3309.

[10] A. Ponrouch, E. Marchante, M. Courty, J.M. Tarascon, M.R. Palacín, In search of an optimized electrolyte for Na-ion batteries, Energy Environ Sci 5 (2012) 8572–8583. https://doi.org/10.1039/c2ee22258b.

[11] Z. Bai, X. Lv, D.H. Liu, D. Dai, J. Gu, L. Yang, Z. Chen, Two-Dimensional NiO@C-N Nanosheets Composite as a Superior Low-Temperature Anode Material for Advanced Lithium-/Sodium-Ion Batteries, ChemElectroChem 7 (2020) 3616–3622. https://doi.org/10.1002/celc.202000747.

[12] Q. Li, D. Yang, H. Chen, X. Lv, Y. Jiang, Y. Feng, X. Rui, Y. Yu, Advances in metal phosphides for sodium-ion batteries, SusMat 1 (2021) 359–392. https://doi.org/10.1002/sus2.19.

[13] B. Song, E. Hu, J. Liu, Y. Zhang, X.Q. Yang, J. Nanda, A. Huq, K. Page, A novel P3-type Na 2/3 Mg 1/3 Mn 2/3 O 2 as high capacity sodium-ion cathode using reversible oxygen redox, J Mater Chem A Mater 7 (2019) 1491–1498. https://doi.org/10.1039/c8ta09422e.

[14] X. Cao, H. Li, Y. Qiao, X. Li, M. Jia, J. Cabana, H. Zhou, Stabilizing Reversible Oxygen Redox Chemistry in Layered Oxides for Sodium-Ion Batteries, Adv Energy Mater 10 (2020). https://doi.org/10.1002/aenm.201903785.

[15] J. Vergnet, M. Saubanère, M.L. Doublet, J.M. Tarascon, The Structural Stability of P2-Layered Na-Based Electrodes during Anionic Redox, Joule 4 (2020) 420–434. https://doi.org/10.1016/j.joule.2019.12.003.

[16] N. Qiu, H. Chen, Z. Yang, S. Sun, Y. Wang, Y. Cui, A high entropy oxide (Mg0.2Co0.2Ni0.2Cu0.2Zn0.2O) with superior lithium storage performance, J Alloys Compd 777 (2019) 767–774. https://doi.org/10.1016/j.jallcom.2018.11.049.

[17] Q. Wang, A. Sarkar, D. Wang, L. Velasco, R. Azmi, S.S. Bhattacharya, T. Bergfeldt, A. Düvel, P. Heitjans, T. Brezesinski, H. Hahn, B. Breitung, Multi-anionic and -cationic compounds: New high entropy materials for advanced Li-ion batteries, Energy Environ Sci 12 (2019) 2433–2442. https://doi.org/10.1039/c9ee00368a.

[18] C.M. Rost, E. Sachet, T. Borman, A. Moballegh, E.C. Dickey, D. Hou, J.L. Jones, S. Curtarolo, J.P. Maria, Entropy-stabilized oxides, Nat Commun 6 (2015). https://doi.org/10.1038/ncomms9485.

[19] R.J. Clément, P.G. Bruce, C.P. Grey, Review—Manganese-Based P2-Type Transition Metal Oxides as Sodium-Ion Battery Cathode Materials, J Electrochem Soc 162 (2015) A2589–A2604. https://doi.org/10.1149/2.0201514jes.

[20] C. Delmas, D. Carlier, M. Guignard, The Layered Oxides in Lithium and Sodium-Ion Batteries: A Solid-State Chemistry Approach, Adv Energy Mater 11 (2021). https://doi.org/10.1002/aenm.202001201.

[21] K. Kang, G. Ceder, Factors that affect Li mobility in layered lithium transition metal oxides, Phys Rev B Condens Matter Mater Phys 74 (2006). https://doi.org/10.1103/PhysRevB.74.094105.

[22] N. Yabuuchi, K. Kubota, M. Dahbi, S. Komaba, Research development on sodium-ion batteries, Chem Rev 114 (2014) 11636–11682. https://doi.org/10.1021/cr500192f.

[23] C. Delmas, C. Fouassier, P. Hagenmuller, STRUCTURAL CLASSIFICATION AND PROPERTIES OF THE LAYERED OXIDES, n.d.

[24] J.B. Goodenough, JAHN-TELLER PHENOMENA IN SOLIDS, 1998.

[25] G.J. Shu, F.C. Chou, Sodium-ion diffusion and ordering in single-crystal P2 -Nax CoO2, Phys Rev B Condens Matter Mater Phys 78 (2008). https://doi.

org/10.1103/PhysRevB.78.052101.

[26] F. Sauvage, L. Laffont, J.M. Tarascon, E. Baudrin, Study of the insertion/deinsertion mechanism of sodium into Na 0.44MnO2, Inorg Chem 46 (2007) 3289–3294. https://doi.org/10.1021/ic0700250.

[27] A.R. Armstrong, M. Holzapfel, P. Nová, C.S. Johnson, S.-H. Kang, M.M. Thackeray, P.G. Bruce, Demonstrating Oxygen Loss and Associated Structural Reorganization in the Lithium Battery Cathode Li[Ni 0.2 Li 0.2 Mn 0.6]O 2, (2006). https://doi.org/10.1021/ja062027.

[28] H. Koga, L. Croguennec, M. Ménétrier, K. Douhil, S. Belin, L. Bourgeois, E. Suard, F. Weill, C. Delmas, Reversible Oxygen Participation to the Redox Processes Revealed for Li 1.20 Mn 0.54 Co0.13 Ni 0.13 O 2 , J Electrochem Soc 160 (2013) A786–A792. https://doi.org/10.1149/2.038306jes.

[29] Y. Wang, E. Wang, X. Zhang, H. Yu, High-Voltage "single-Crystal" Cathode Materials for Lithium-Ion Batteries, Energy and Fuels 35 (2021) 1918–1932. https://doi.org/10.1021/acs.energyfuels.0c03608.

[30] R.A. House, J.J. Marie, J. Park, G.J. Rees, S. Agrestini, A. Nag, M. Garcia-Fernandez, K.J. Zhou, P.G. Bruce, Covalency does not suppress O2 formation in 4d and 5d Li-rich O-redox cathodes, Nat Commun 12 (2021). https://doi.org/10.1038/s41467-021-23154-4.

[31] R.A. House, J.J. Marie, M.A. Pérez-Osorio, G.J. Rees, E. Boivin, P.G. Bruce, The role of O2 in O-redox cathodes for Li-ion batteries, Nat Energy 6 (2021) 781–789. https://doi.org/10.1038/s41560-021-00780-2.

[32] R.A. House, G.J. Rees, M.A. Pérez-Osorio, J.J. Marie, E. Boivin, A.W. Robertson, A. Nag, M. Garcia-Fernandez, K.J. Zhou, P.G. Bruce, First-cycle voltage hysteresis in Li-rich 3d cathodes associated with molecular O2 trapped in the bulk, Nat Energy 5 (2020) 777–785. https://doi.org/10.1038/s41560-020-00697-2.

[33] P.M. Csernica, S.S. Kalirai, W.E. Gent, K. Lim, Y.S. Yu, Y. Liu, S.J. Ahn, E. Kaeli, X. Xu, K.H. Stone, A.F. Marshall, R. Sinclair, D.A. Shapiro, M.F. Toney, W.C. Chueh, Persistent and partially mobile oxygen vacancies in Li-rich layered oxides, Nat Energy 6 (2021) 642–652. https://doi.org/10.1038/s41560-021-00832-7.

[34] P. Yan, J. Zheng, Z.K. Tang, A. Devaraj, G. Chen, K. Amine, J.G. Zhang, L.M. Liu, C. Wang, Injection of oxygen vacancies in the bulk lattice of layered cathodes, Nat Nanotechnol 14 (2019) 602–608. https://doi.org/10.1038/s41565-019-0428-8.

[35] N. Yabuuchi, R. Hara, M. Kajiyama, K. Kubota, T. Ishigaki, A. Hoshikawa, S. Komaba, New O2/P2-type Li-excess layered manganese oxides as promising multi-functional electrode materials for rechargeable Li/Na batteries, Adv Energy Mater 4 (2014). https://doi.org/10.1002/aenm.201301453.

[36] R. Berthelot, D. Carlier, C. Delmas, Electrochemical investigation of the P2-NaxCoO2 phase diagram, Nat Mater 10 (2011) 74–80. https://doi.org/10.1038/nmat2920.

[37] M. Guignard, C. Didier, J. Darriet, P. Bordet, E. Elkaïm, C. Delmas, P2-Na x VO 2 system as electrodes for batteries and electron-correlated materials, Nat Mater 12 (2013) 74–80. https://doi.org/10.1038/nmat3478.

[38] J. Xu, H. Liu, Y.S. Meng, Exploring Li substituted O3-structured layered oxides NaLixNi1/3 - XMn1/3 + xCo1/3 - XO2 (x = 0.07, 0.13, and 0.2) as promising cathode materials for rechargeable Na batteries, Electrochem Commun 60 (2015) 13–16. https://doi.org/10.1016/j.elecom.2015.07.023.

[39] N.K. Karan, M.D. Slater, F. Dogan, D. Kim, C.S. Johnson, M. Balasubramanian, Operando Structural Characterization of the Lithium-Substituted Layered Sodium-Ion Cathode Material P2-Na 0.85 Li 0.17 Ni 0.21 Mn 0.64 O 2 by X-ray Absorption Spectroscopy, J Electrochem Soc 161 (2014) A1107–A1115. https://doi.org/10.1149/2.088406jes.

[40] D. Kim, S.H. Kang, M. Slater, S. Rood, J.T. Vaughey, N. Karan, M. Balasubramanian, C.S. Johnson,

Enabling sodium batteries using lithium-substituted sodium layered transition metal oxide cathodes, Adv Energy Mater 1 (2011) 333–336. https://doi.org/10.1002/aenm.201000061.

[41] A. Mendiboure, C. Delmas, P. Hagenmuller, Electrochemical Intercalation and Deintercalation of NaxMnOz Bronzes, 1985.

[42] J.-P. Parant, R. Olazcuaga, M. Devalette, C. Fouassier, Sur Quelques Nouvelles Phases de Formule Na,MnO, (x G 1), 1971.

[43] J. Cabana, N.A. Chernova, J. Xiao, M. Roppolo, K.A. Aldi, M.S. Whittingham, C.P. Grey, Study of the transition metal ordering in layered NaxNi x/2Mn1-x/2O2 (2/3 ≤ x ≤ 1) and consequences of Na/Li exchange, Inorg Chem 52 (2013) 8540–8550. https://doi.org/10.1021/ic400579w.

[44] D. Buchholz, C. Vaalma, L.G. Chagas, S. Passerini, Mg-doping for improved long-term cyclability of layered Na-ion cathode materials - The example of P2-type NaxMg0.11Mn0.89O2, J Power Sources 282 (2015) 581–585. https://doi.org/10.1016/j.jpowsour.2015.02.069.

[45] R.J. Clément, D. Kitchaev, J. Lee, Gerbrand Ceder, Short-Range Order and Unusual Modes of Nickel Redox in a Fluorine-Substituted Disordered Rocksalt Oxide Lithium-Ion Cathode, Chemistry of Materials 30 (2018) 6945–6956. https://doi.org/10.1021/acs.chemmater.8b03794.

[46] N.K. Karan, M.D. Slater, F. Dogan, D. Kim, C.S. Johnson, M. Balasubramanian, Operando Structural Characterization of the Lithium-Substituted Layered Sodium-Ion Cathode Material P2-Na 0.85 Li 0.17 Ni 0.21Mn0.64O2 by X-ray Absorption Spectroscopy, J Electrochem Soc 161 (2014) A1107–A1115. https://doi.org/10.1149/2.088406jes.

[47] D. Kim, S.H. Kang, M. Slater, S. Rood, J.T. Vaughey, N. Karan, M. Balasubramanian, C.S. Johnson, Enabling sodium batteries using lithium-substituted sodium layered transition metal oxide cathodes, Adv Energy Mater 1 (2011) 333–336. https://doi.org/10.1002/aenm.201000061.

[48] I. Hasa, D. Buchholz, S. Passerini, J. Hassoun, A comparative study of layered transition metal oxide cathodes for application in sodium-ion battery, ACS Appl Mater Interfaces 7 (2015) 5206–5212. https://doi.org/10.1021/am5080437.

[49] J. Billaud, G. Singh, A.R. Armstrong, E. Gonzalo, V. Roddatis, M. Armand, T. Rojo, P.G. Bruce, Na0.67Mn1-xMgxO2 (0 ≤ x ≤ 0.2): A high capacity cathode for sodium-ion batteries, in: Energy Environ Sci, Royal Society of Chemistry, 2014: pp. 1387–1391. https://doi.org/10.1039/c4ee00465e.

[50] N. Yabuuchi, R. Hara, M. Kajiyama, K. Kubota, T. Ishigaki, A. Hoshikawa, S. Komaba, New O2/P2-type Li-excess layered manganese oxides as promising multi-functional electrode materials for rechargeable Li/Na batteries, Adv Energy Mater 4 (2014). https://doi.org/10.1002/aenm.201301453.

[51] N. Yabuuchi, H. Yoshida, S. Komaba, Crystal structures and electrode performance of alpha-NaFeO2 for rechargeable sodium batteries, Electrochemistry 80 (2012) 716–719. https://doi.org/10.5796/electrochemistry.80.716.

[52] Z. Lu, J.R. Dahn, In Situ X-Ray Diffraction Study of P2-Na[sub 2/3][Ni[sub 1/3]Mn[sub 2/3]]O[sub 2], J Electrochem Soc 148 (2001) A1225. https://doi.org/10.1149/1.1407247.

[53] A. Caballero, L. Hernán, J. Morales, L. Sánchez, J. Santos Peña, M.A.G. Aranda, Synthesis and characterization of high-temperature hexagonal P2-Na0.6 Mno_2 and its electrochemical behaviour as cathode in sodium cells, J Mater Chem 12 (2002) 1142–1147. https://doi.org/10.1039/b108830k.

[54] PII: S0167-2738(99)00147-2, 1999. www.elsevier.com/locate/ssi.

[55] Herbert B. Callen - Thermodynamics and an Introduction to Thermostatistics-Wiley (1985), (n.d.).

[56] B.S. Murty, J.W. Yeh, S. Ranganathan, P.P. Bhattacharjee, High-entropy alloys: basic concepts, in: High-Entropy Alloys, Elsevier, 2019: pp. 13–30. https://doi.org/10.1016/b978-0-12-816067-1.00002-3.

[57] B.S. Murty, J.W. Yeh, S. Ranganathan, A Brief History of Alloys and the Birth of High-Entropy Alloys, in: High Entropy Alloys, Elsevier, 2014: pp. 1–12. https://doi.org/10.1016/b978-0-12-800251-3.00001-8.

[58] B. Cantor, I.T.H. Chang, P. Knight, A.J.B. Vincent, Microstructural development in equiatomic multicomponent alloys, Materials Science and Engineering: A 375–377 (2004) 213–218. https://doi.org/10.1016/j.msea.2003.10.257.

[59] J.W. Yeh, S.K. Chen, S.J. Lin, J.Y. Gan, T.S. Chin, T.T. Shun, C.H. Tsau, S.Y. Chang, Nanostructured high-entropy alloys with multiple principal elements: Novel alloy design concepts and outcomes, Adv Eng Mater 6 (2004) 299–303. https://doi.org/10.1002/adem.200300567.

[60] K. Liu, S.S. Nene, M. Frank, S. Sinha, R.S. Mishra, Extremely high fatigue resistance in an ultrafine grained high entropy alloy, Appl Mater Today 15 (2019) 525–530. https://doi.org/10.1016/j.apmt.2019.04.001.

[61] S.S. Nene, Some Distinct Features of Transformative High Entropy Alloys for Metal Additive Manufacturing, Front Mater 9 (2022). https://doi.org/10.3389/fmats.2022.873911.

[62] D.B. Miracle, O.N. Senkov, A critical review of high entropy alloys and related concepts, Acta Mater 122 (2017) 448–511. https://doi.org/10.1016/j.actamat.2016.08.081.

[63] A. Manzoor, S. Pandey, D. Chakraborty, S.R. Phillpot, D.S. Aidhy, Entropy contributions to phase stability in binary random solid solutions, NPJ Comput Mater 4 (2018). https://doi.org/10.1038/s41524-018-0102-y.

[64] J.W. Yeh, Alloy design strategies and future trends in high-entropy alloys, JOM 65 (2013) 1759–1771. https://doi.org/10.1007/s11837-013-0761-6.

[65] H. Gao, J. Li, F. Zhang, C. Li, J. Xiao, X. Nie, G. Zhang, Y. Xiao, D. Zhang, X. Guo, Y. Wang, Y.M. Kang, G. Wang, H. Liu, Revealing the Potential and Challenges of High-Entropy Layered Cathodes for Sodium-Based Energy Storage, Adv Energy Mater 14 (2024). https://doi.org/10.1002/aenm.202304529.

[66] Y. Chen, H. Fu, Y. Huang, L. Huang, X. Zheng, Y. Dai, Y. Huang, W. Luo, Opportunities for High-Entropy Materials in Rechargeable Batteries, ACS Mater Lett 3 (2021) 160–170. https://doi.org/10.1021/acsmaterialslett.0c00484.

[67] R. Guo, L. Yu, Z. Liu, J. Pan, Y. Yao, L. Liu, Enthalpy induced phase partition toward hierarchical, nanostructured high-entropy alloys, Nano Res 15 (2022) 4893–4901. https://doi.org/10.1007/s12274-021-3912-z.

[68] M.C. Troparevsky, J.R. Morris, P.R.C. Kent, A.R. Lupini, G.M. Stocks, Criteria for predicting the formation of single-phase high-entropy alloys, Phys Rev X 5 (2015). https://doi.org/10.1103/PhysRevX.5.011041.

[69] Y. Yao, Q. Dong, A. Brozena, J. Luo, J. Miao, M. Chi, C. Wang, I.G. Kevrekidis, Z.J. Ren, J. Greeley, G. Wang, A. Anapolsky, L. Hu, High-entropy nanoparticles: Synthesis-structureproperty relationships and data-driven discovery, Science (1979) 376 (2022). https://doi.org/10.1126/science.abn3103.

[70] J. Wang, S.L. Dreyer, K. Wang, Z. Ding, T. Diemant, G. Karkera, Y. Ma, A. Sarkar, B. Zhou, M. V. Gorbunov, A. Omar, D. Mikhailova, V. Presser, M. Fichtner, H. Hahn, T. Brezesinski, B. Breitung, Q. Wang, P2-type layered high-entropy oxides as sodium-ion cathode materials, Materials Futures 1 (2022). https://doi.org/10.1088/2752-5724/ac8ab9.

[71] S.L. Dreyer, R. Zhang, J. Wang, A. Kondrakov, Q. Wang, T. Brezesinski, J. Janek, The effect of configurational entropy on acoustic emission of P2-type layered oxide cathodes for sodium-ion batteries, JPhys

Energy 5 (2023). https://doi.org/10.1088/2515-7655/acd41a.

[72] Q. Shen, Y. Liu, X. Zhao, J. Jin, X. Song, Y. Wang, X. Qu, L. Jiao, Unexpectedly High Cycling Stability Induced by a High Charge Cut-Off Voltage of Layered Sodium Oxide Cathodes, Adv Energy Mater 13 (2023). https://doi.org/10.1002/aenm.202203216.

[73] J. Jin, Y. Liu, Q. Shen, X. Zhao, J. Zhang, Y. Song, T. Li, X. Xing, J. Chen, Unveiling the Complementary Manganese and Oxygen Redox Chemistry for Stabilizing the Sodium-Ion Storage Behaviors of Layered Oxide Cathodes, Adv Funct Mater 32 (2022). https://doi.org/10.1002/adfm.202203424.

[74] F. Fu, X. Liu, X. Fu, H. Chen, L. Huang, J. Fan, J. Le, Q. Wang, W. Yang, Y. Ren, K. Amine, S.G. Sun, G.L. Xu, Entropy and crystal-facet modulation of P2-type layered cathodes for long-lasting sodium-based batteries, Nat Commun 13 (2022). https://doi.org/10.1038/s41467-022-30113-0.

[75] S. Ma, P. Zou, H.L. Xin, Extending phase-variation voltage zones in P2-type sodium cathodes through high-entropy doping for enhanced cycling stability and rate capability, Mater Today Energy 38 (2023). https://doi.org/10.1016/j.mtener.2023.101446.

[76] S. Yan, S. Luo, L. Yang, J. Feng, P. Li, Q. Wang, Y. Zhang, X. Liu, Novel P2-type layered medium-entropy ceramics oxide as cathode material for sodium-ion batteries, Journal of Advanced Ceramics 11 (2022) 158–171. https://doi.org/10.1007/s40145-021-0524-8.

[77] H. Liu, Y. Wang, X. Ding, Y. Wang, F. Wu, H. Gao, A high-entropy layered P2-type cathode with high stability for sodium-ion batteries, Sustain Energy Fuels 8 (2024) 1304–1313. https://doi.org/10.1039/d3se01597a.